Use of RAD sequencing for delimiting species

Eric Pante, Jawad Abdelkrim, Amélia Viricel, Delphine Gey, Scott France, Marie-Catherine Boisselier, Sarah Samadi

Heredity – Original Article

Use of RAD sequencing for delimiting species

Pante E[1], Abdelkrim J[2*], Viricel A[1*], Gey D[2], France S[3], Boisselier MC[2,4], Samadi S[4]

[1] Laboratoire LIENSs, UMR 7266 CNRS - Université de La Rochelle, La Rochelle, France

[2] Département Systématique et Evolution, UMS 2700 MNHN-CNRS, SSM, Muséum national d'Histoire naturelle, Paris, France

[3] Department of Biology, University of Louisiana at Lafayette, Lafayette LA, USA

[4] ISYEB – UMR 7205 – CNRS, MNHN, UPMC, EPHE, Muséum national d'Histoire naturelle, Sorbonne Universités, Paris

[*] authors contributed equally to the work

Corresponding author:

Eric Pante, Laboratoire LIENSs, UMR 7266 CNRS - Université de La Rochelle, La Rochelle, France. Tel: +33 05 46 50 76 37; Fax: +33 05 46 50 76 63; Email: pante.eric@gmail.com

Running title: Use of RAD sequencing for delimiting species

Word count: 6 999 words

Abstract

RAD-tag sequencing is a promising method for conducting genome-wide evolutionary studies. However, to date, only a handful of studies empirically tested its applicability above the species level. In this communication, we use RAD-tags to contribute to the delimitation of species within a diverse genus of deep-sea octocorals, *Chrysogorgia*, for which few classical genetic markers have proved informative. Previous studies have hypothesized that single mitochondrial haplotypes can be used to delimit *Chrysogorgia* species. Based on two lanes of Illumina sequencing, we inferred phylogenetic relationships among twelve putative species that were delimited using mitochondrial data, comparing two RAD analysis pipelines (Stacks and pyRAD). The number of homologous RAD loci decreased dramatically with increasing divergence, as >70% of loci are lost when comparing specimens separated by two mutations on the 700 nt long mitochondrial phylogeny. Species delimitation hypotheses based on the mitochondrial *mtMutS* gene are largely supported, as six out of nine putative species represented by more than one colony were recovered as discrete, well-supported clades. Significant genetic structure (correlating with geography) was detected within one putative species, suggesting that individuals characterized by the same *mtMutS* haplotype may belong to distinct species. Conversely, three *mtMutS* haplotypes formed one well-supported clade within which no population structure was detected, also suggesting that intra-specific variation exists at *mtMutS* in *Chrysogorgia*. Despite an impressive decrease in the number of homologous loci across clades, RAD data helped us to fine-tune our interpretations of classical mitochondrial markers used in octocoral species delimitation, and discover previously undetected diversity.

Keywords (3-6): phylogenomics, octocoral, Stacks, PyRAD, SNP, species delimitation

Introduction

The advent of next-generation sequencing tools has permitted significant advances in our understanding of evolutionary processes such as speciation (e.g. Ekblom and Galindo 2011), but some other practical applications of genomic data have been less explored, including phylogenomics and species delimitation. Among genomic approaches that are applicable to these fields, the usefulness of restriction-site-associated DNA tag (RAD-tag; Baird *et al.,* 2008) sequencing has been investigated in few studies to date. This methodology typically provides short sequences (~ 100-150 bp) flanking the cut sites of a restriction enzyme (or several enzymes), generally yielding thousands of loci distributed throughout the genome. This approach does not require a reference genome, and can therefore be applied to non-model organisms. However, some technical difficulties remain for groups where very little genomic knowledge is available (see Davey *et al.,* 2011). For instance, the choice of restriction enzyme(s) and methodology (single-digest versus double-digest RAD) is key to estimating the number of expected cut sites and coverage, but relies on prior knowledge of genome size and GC content.

Despite these difficulties, RAD-tag sequencing constitutes one of the reduced genomic approaches that are suitable for investigating inter-specific evolutionary questions. Published RAD-tag sequencing research beyond the species level includes *in silico* studies (*Drosophila*, mammals, and yeasts in Rubin *et al.,* 2012; *Drosophila* in Cariou *et al.,* 2013) and empirical work (e.g. Restionaceae flowering plants in Lexer *et al.,* 2013; cetaceans in Viricel *et al.,* 2014), which both suggest this approach is promising for taxa having diverged up to 60 million years ago. For

74 instance, RAD-tag sequencing has proven useful in species delimitation and
75 phylogenies within recently and rapidly diverged groups (e.g. Orobanchaceae
76 flowering plants in Eaton and Ree 2013; swordtails in Jones *et al.,* 2013; *Heliconius*
77 butterflies in Nadeau *et al.,* 2013; cichlids in Wagner *et al.,* 2013; geckos in Leaché *et*
78 *al*., 2014). Comparatively, reconstructing the phylogeny of more distantly related taxa
79 has been the topic of a single study (*Carabus* beetles, Cruaud *et al.,* 2014), to the best
80 of our knowledge. Herein we use this approach on a group of deep-sea octocorals for
81 which little genomic data are available. Thus, our contribution constitutes one of the
82 first studies investigating the use of RAD-tag sequencing for practical species
83 delimitation within a taxonomic group composed of divergent species (up to 16
84 million years ago).

85 Deep-sea octocorals are one of the groups for which RAD-tag sequencing can
86 significantly advance our understanding of evolutionary patterns. As for shallow-
87 water octocorals, deep-water octocorals present significant challenges for
88 taxonomists, with few morphological characters being available for species
89 delimitation (e.g., McFadden *et al.,* 2010). In addition, several studies have shown
90 conflicting patterns of morphological and molecular data (France 2007; Dueñas and
91 Sánchez 2009; Pante and France 2010), suggesting that an integrative approach to
92 taxon delimitation must be applied in this group (e.g. Schlick-Steiner *et al*., 2010).
93 Octocorals, as with other anthozoans (e.g. scleractinians and sea anemones), are also
94 plagued with remarkably low levels of mitochondrial genome evolution that renders
95 the use of classical barcoding gene regions such as *cox1* of limited use (McFadden *et*
96 *al.,* 2011). Comparatively, a few studies have successfully used nuclear markers within
97 octocoral species (e.g. Concepcion *et al.,* 2008; Mokhtar-Jamaï *et al.,* 2011), but these
98 are either not widely useable across octocorals (e.g. SRP54; France and Pante
99 unpublished observations), or not informative at multiple phylogenetic scales (e.g.

100 microsatellites). Multi-copy markers have been employed (e.g. Herrera *et al.,* 2010),
101 however their use implies that lack of concerted evolution within and across genomes
102 will not blur the phylogenetic signal (Vollmer and Palumbi 2004; Calderón et al 2006).
103 In this group, RAD-tag genotyping may therefore offer a panel of markers to help
104 describe patterns of population structure, delimit species, and investigate
105 phylogenetic relationships. This technique may however be difficult to implement in
106 this group. Indeed, the composition of the deep-sea octocoral genome is unknown
107 (size, GC content, prevalence of cut sites for restriction enzymes, etc.); the size of
108 known cnidarian genomes, for instance, varies between 224 Mb and 1.8 Tb (Animal
109 Genome Size Database; Gregory, 2014). In addition, sampling of deep-sea animals can
110 be associated with a loss of quality of genomic DNA samples, particularly when
111 sampling in tropical waters using trawls or dredges.

112 The genus *Chrysogorgia* (Calcaxonia: Chrysogorgiidae) is a noteworthy model
113 for testing the utility of RAD sequencing for delimiting octocoral species, as it is
114 diverse (62 nominal species described, 93% of which were based solely on
115 morphology), widely distributed, and can be locally abundant (Watling *et al.,* 2011).
116 The large geographic, bathymetric, and ecological distributions of
117 some *Chrysogorgia* species (Pante *et al.,* 2012b) question whether taxa are
118 appropriately delimited, and whether cryptic diversity is important in the group. In
119 the northwestern Atlantic, congruence exists between morphological and genetic data,
120 suggesting that a relatively short fragment of the mitochondrial *mtMutS* gene can be
121 used to formulate "Primary Species Hypotheses" (Pante and Watling 2012). It is
122 suspected that little to no intra-specific variation exists for this marker within the
123 group (McFadden *et al.,* 2011), but the null hypothesis that single mutations
124 at *mtMutS* are diagnostic of species limits must be evaluated using genetic data from

125 markers informative within and above the species level. RAD loci allow to test
126 whether lineages that putatively belong to different species do not exchange genes.

127 In this communication we test the utility of RAD-tag genotyping for delimiting
128 species in *Chrysogorgia* using the genealogical criterion defined by Taylor *et al*.,
129 (2001). More specifically, we test whether single mutations on the mitochondrial
130 *mtMutS* gene can be used as a criterion for grouping *Chrysogorgia* colonies into
131 separate, putative species (or, more specifically, "Primary Species Delimitation
132 hypotheses" as in Puillandre *et al*., 2012). We compare the results from two analysis
133 pipelines, Stacks (Catchen *et al.,* 2013) and PyRAD (Eaton, 2014), which significantly
134 differ in the method employed for detecting homologous loci.

135

136 **Material and methods**

137 *Specimen collection and mtDNA typing*

138 *Chrysogorgia* specimens were collected from the SE slope of New Caledonia (NC) and
139 adjacent seamounts of the Norfolk Ridge (82 colonies; *Terrasses* cruise, 2008), from
140 Papua New Guinea (PNG; 8 colonies; *BioPapua* cruise, 2010), and from the
141 northwestern Atlantic (1 colony, *Extreme Coral 2010* cruise; Tables 1 and S1). Pacific
142 specimens were retrieved from dredges and trawls (details on cruises of the Tropical
143 Deep Sea Benthos research program: Bouchet *et al.,* 2008; details on the *BioPapua*
144 cruise: Pante *et al.,* 2012a); the Atlantic specimen was collected using the Jason II ROV
145 (Woods Hole Oceanographic Institution). Specimens were fixed in 80% ethanol as
146 soon as possible after collection. Genomic DNA was extracted using a CTAB protocol
147 according to France *et al.* (1996). A 700-bp fragment of the mitochondrial *mtMutS*

148 gene (identified as more informative than *cox1* or 18S in chrysogorgiids, Pante *et al*.,
149 2012b) was amplified using the ND4L2475F – MUT3458R primer pair and sequenced
150 using an ABI PRISM (R) 3100 or 3130xl Genetic Analyzer (primer information, PCR
151 and sequencing conditions: Pante *et al.,* 2012b). Sequences were checked for quality
152 and edited in Sequencher (TM) 4.7 (Gene Codes), aligned by eye (a single, 3 bp indel
153 was present in the alignment), and haplotypes were submitted to GenBank (Table S1).
154 Divergence times among putative species were estimated using the molecular clock
155 from Lepard (2003), which was calculated for the shallow-water octocoral genus
156 *Lepogorgia* based on *mtMutS* genetic distances for clades located on either sides of the
157 Isthmus of Panama (0.14–0.25%/million years).

158 *Library construction, RAD sequencing, and quality control*

159 Genomic DNA quality was evaluated by 1% agarose gel electrophoresis, and
160 quantified using a Thermo Scientific Nanodrop ND-1 000 spectrophotometer. DNA
161 was sent to Eurofins Genomics (Ebersberg, Germany) for RAD-tag library preparation
162 and sequencing. Libraries were constructed from 1-2 µg of DNA per colony using the
163 *SbfI* restriction enzyme. This enzyme was chosen because it was successfully used in
164 RADseq experiments with marine invertebrates (sea-anemones, Reitzel *et al*., 2013;
165 abalone, Gruenthal *et al*., 2014), and was expected to allow an acceptable compromise
166 between prevalence of cut sites and depth of coverage, based on RADcounter (the
167 University of Edinburgh, https://www.wiki.ed.ac.uk/display/RADSequencing/Home).
168 As the genome size and GC content of *Chrysogorgia* (or other octocorals, to the best of
169 our knowledge) are not known, we estimated the prevalence of S*bfI* cut sites based on
170 a range of genome sizes and GC content, based on information from the Animal
171 Genome Size Database (see Introduction) and with a GC content of 40% (e.g. Soza-
172 Ried *et al.*, 2009). Barcodes 6-9 nucleotides long and differing by at least 2 nucleotides

were used to differentiate multiplexed samples (Table S1). Sequencing was performed on two lanes of the Illumina (R) HiSeq (TM) 2 000 instrument (Illumina Inc., San Diego CA, USA) using the single read, 100 nucleotide configuration. Raw HiSeq output was processed using the CASAVA v1.8.2 software pipeline (Illumina Inc., San Diego CA, USA), and de-multiplexed and quality filtered using the process_radtags.pl module (default quality settings) of the Stacks v.0.99994 pipeline (Catchen *et al.,* 2013). A single sequencing error was tolerated in the barcode. Reads were truncated to 91 nucleotides. Quality (as measured by phred scores and percentage of sequence overrepresentation) was checked before and after treatment by process_radtags using FastQC v.0.10.1 (http://www.bioinformatics.babraham.ac.uk/projects/fastqc/).

Exploration of the divergence parameter space

Two main pipelines specifically designed for analysis of RADseq data are currently available. The most used to date is the Stacks pipeline. It constructs a catalog of loci for a set of samples mainly based on three parameters: the minimum stack depth parameter m (i.e. the minimum number of reads allowed per allele), the intra-individual divergence parameter M (i.e. the maximum number of mutations that can be observed between stacks within a sample), and the inter-individual divergence parameter n (i.e. the maximum number of mutations that can be observed between loci across samples).

PyRAD (Eaton 2014) is a more recently developed pipeline and differs from Stacks in several ways, the most important one being that it allows the presence of indels, since the clustering process of reads into loci uses alignment tools. This is anticipated to be an advantage compared to the first pipeline when considering more phylogenetically distant species. PyRAD relies on a large number of parameters used at different steps of the process. Most of them are related to reads quality control,

198 detection of homology and filtering of paralogs. Two main parameters are of
199 particular importance: the minimum depth coverage Mindepth (minimum depth
200 necessary to make a statistical base call at each position of a cluster) and the similarity
201 threshold Wclust (similarity value to be used for the alignment during both the within
202 and across-sample clustering).

203 For both pipelines, these parameter settings are expected to influence greatly
204 the number of markers available for intra- and inter-specific comparisons and it is
205 necessary to explore which parameter combinations maximize the number of
206 orthologous loci (Viricel *et al.,* 2014). To explore the effect of these parameters at
207 different phylogenetic depths, we randomly selected pairs of specimens that (1) were
208 separated by 0 to 16 mutations at *mtMutS* (representing different levels of
209 phylogenetic divergence), and (2) were characterized by 1 to 1.5 million reads (to
210 alleviate potential effects of depth of coverage on the number of assembled loci). For
211 each level of divergence, we used three replicate pairs of specimens. We refer to
212 specimens with *mtMutS* haplotypes differing by few mutations as pairs of closely-
213 related colonies, and those with haplotypes differing by many mutations as distantly-
214 related colonies.

215 In Stacks, m was kept to 3 (the default value); M was incremented from 1 to
216 10 in two cases (specimens separated by 0 and 12 mutations at *mtMutS*), and from 1
217 to 7 in all other cases. Similarly, n was incremented from 1 to 10 (0 and 12 mutations
218 cases) and from 1 to 8 (all cases). All combinations of M and n were not tested: only
219 similar values of M and n were used together (two settings were used: M=n and
220 M+1=n), as to (1) keep maximum levels of intra- and inter-individual divergence
221 levels close, and (2) keep the number of Stacks analyses to a reasonable number. A
222 total of 408 Stacks catalog construction tests were therefore performed using the

223 denovo_map.pl script available in Stacks. Catalogs were parsed with the populations.pl
224 script, where each sample was considered as a separate population, no missing data
225 were allowed, and a minimum of 10 reads per SNP was set.

226 In PyRAD v. 2.0, combinations of two values for Mindepth (3 and 6) and 3
227 values for Wclust (0.89, 0.93 and 0.96) were tested, resulting in 156 analyses. For
228 these analyses, the maximum number of sites per read with a quality < 20 (NQual)
229 was set to 4, the minimum number of samples in a final locus (MinCov) was set to 1
230 and the maximum proportion of shared polymorphic sites in a locus (MaxSH) was set
231 to 10%. For this last parameter, which aims at detecting paralogs, preliminary tests
232 showed that in our case, changing this value did not drastically affect the number of
233 loci and SNPs detected. Finally, optional parameters were kept to default values.

234 *Comparison of Stacks and PyRAD*

235 To evaluate what proportion of loci was detected by both PyRAD and Stacks, a custom
236 BLASTN search was performed (BLAST toolkit v. 2.2.25; Zhang *et al.,* 2000). Local
237 BLAST databases were constructed using PyRAD sequences (locus file containing
238 consensus sequences for each individual; PyRAD parameters m=6 and Wclust=93%
239 and 89%) for three groups of specimens with different numbers of reads (Table 2).
240 Stacks loci for these specimens (based on the locus file produced by the populations
241 script, for which a single allele was retained per locus; denovo_map parameters m=3,
242 M=4, n=4, and m=3, M=10, n=12) were then compared to the PyRAD database using
243 BLASTN (percent identity set to 93% and 89%, word size 80 and 84 nt, ungapped
244 alignments). The XML output of BLASTN searches was then parsed in bash using grep.

245 *Phylogenetic reconstruction and species delimitation*

246 RAxML v. 8.0.9 (Stamatakis 2006; Stamatakis *et al.,* 2008) was used on the

CIPRES Portal (Miller *et al.,* 2010) to infer phylogenetic relationships among *Chrysogorgia* colonies, based on mitochondrial and nuclear sequences, using the GTRCATI model and automating boot-stopping. The mitochondrial phylogeny was inferred from the first 700 nt of the *mtMutS* gene (see above); the nuclear phylogeny was inferred using concatenated RAD loci obtained based on two parameter sets in Stacks, and one parameter set in PyRAD. The first Stacks set ("m3M4n4", denovo_map parameters m=3, M=4, n=4; populations script parameters m=6, p=2, r=0.5) corresponds to parameters that maximize the total number of loci detected while minimizing divergence parameters (see "Exploration of the divergence parameter space" section above). For this analysis, each *mtMutS* haplotype was considered as a separate population. The Stacks populations script parameters that were used signify that 50% missing data were allowed within each population, a locus had to be present in at least two populations to be included in the output and a minimum of 6 reads per SNP was required. The second Stacks set ("m3M10n12", Stacks script denovo_map parameters m=3, M=10, n=12; populations script parameters m=6, p=2, r=0.5) allowed more divergence between loci. The PyRAD dataset ("m6s93") was constructed with m=6 and Wclust=93% (details above). In all analyses, the Atlantic colony JAC1018 was used as the outgroup.

Once clades were delimited with RAxML, a Discriminant Analysis on Principal Components (DAPC, Jombart *et al.,* 2010) was used to explore genetic structure within three clades represented by 18 to 31 colonies (see below). This method takes into account the multilocus genotype of each individual and forms clusters based on genetic similarity without considering a model of evolution. We also used TESS (Durand *et al*., 2009) to investigate population structure using the conditional auto-correlative (CAR) admixture model with a spatially explicit, Bayesian framework. In TESS, the Deviance Information Criterion (DIC) was used to compare

273 population structure in the presence of different numbers of clusters (the maximum
274 number of cluster K was set to the total number of individual in the tested clade; for
275 example, K was set from 2 to 18 for clade 1). Five replicate runs were used per K, with
276 1 200 MCMC steps and a 200-step burnin. The best K was determined by minimizing
277 DIC and its variance; once the best K determined, a longer analysis with 12 000 steps
278 and a 2 000-step burnin was run to obtain reliable individual assignments. The
279 populations script in Stacks was re-run to keep only one SNP per locus, in order to
280 minimize the probability of co-analyzing linked markers. The Stacks m3M4n4 dataset
281 was chosen for these analyses for two reasons: (1) the DAPC and TESS analyses are
282 run within clades at shallow phylogenetic depths, and (2) as only one SNP / locus is
283 retained, divergence level should be kept minimal to prevent the inclusion of non-
284 homologous loci. The DAPC analysis was run using adegenet in R (Jombart 2008; R
285 Development Core Team 2014).

286

287 **Results**

288

289 *Mitochondrial typing and RAD-tag sequencing*

290

291 A total of 12 *mtMutS* haplotypes were detected among the 91 colonies investigated, 10
292 of which were from NC, 3 from PNG, 1 from the northwestern Atlantic, and 2 being
293 shared between NC and PNG. The biogeography of these mitochondrial haplotypes at
294 these locations is further discussed in Pante *et al.* (2012ab). A total of 236 million raw
295 reads, corresponding to 35 463 Mbp were produced on two HiSeq2000 lanes. The
296 number of quality-filtered reads (in millions) per colony varied between 0.04
297 (TER11108) and 5.82 (TER2044), with a median of 1.6. There was a significant
298 correlation between the number of quality-filtered reads per colony and haplotypes

(Kruskal-Wallis chi-squared = 25.11, df = 13, p-value = 0.02), haplotypes 6 and 10, for instance, yielded fewer reads than other haplotypes (haplotype 10 colonies were sampled from depths down to 880 m, and haplotype 6 colonies had remarkably small polyps that may have been particularly sensitive to prolonged times to preservation).

Loci, SNPs, and indel cataloguing using Stacks and PyRAD

Results from both pipelines (Stacks and PyRAD) show variations in the number of loci and SNPs depending on the set of parameters used (Figure 1a-e, 1g-k), as well as the mitochondrial genetic distance between samples (Figure 1f). For Stacks, as the mitochondrial genetic distance among included samples decreases, both the total number of loci and the number of polymorphic loci increases (Figure 1ab). The former ranges from a few loci to more than 2 000, whereas the latter ranges from a few loci to ~1 000, depending on the set of parameters used. When related to time of divergence (in MY, based on mtDNA), the total number of loci obtained decreases exponentially (Figure 1f). Inversely, the percentage of polymorphic loci is lower for more closely-related colonies (~40%) than for distantly related-colonies (~90%; Figure 1c). These three measures (number of loci, number of polymorphic loci and percentage of polymorphic loci) show the same response to an increase in divergence parameters M and n, namely a rapid increase followed by a plateau. This plateau is reached for the m3M4n4 set of parameters. Conversely, the number of SNPs increases drastically without reaching a plateau, from a few SNPs for the most stringent set of parameters and the most distantly-related colonies to around 3 000 for the most closely-related colonies and the most relaxed set of parameters (Figure 1d). Thus, the effect of increasing mitochondrial genetic distance among samples or decreasing stringency of

parameters is to increase SNPs densities, from one SNP every 250 bp to one SNP every 20 bp (Figure 1e).

Results of the PyRAD analyses follow the general trends observed for the Stacks pipeline. These trends are an increase in total number of loci and polymorphic loci (Figure 1gh) for more relaxed parameters sets, as well as for more closely-related colonies. As for Stacks, more distantly-related specimen pairs have fewer loci than for closely-related ones, but a larger proportion of those is polymorphic (Figure 1i). While the percentage of polymorphic loci shows similar ranges of values for Stacks and PyRAD, the total number of loci as well as the number of polymorphic loci are almost doubled (from 2 000 to almost 4 000 and from 1 000 to almost 2 000, respectively). The same pattern is observed for the number of SNPs and SNP densities (Figure 1jk): PyRAD output differs from Stacks output by a factor of almost two, resulting in SNPs densities twice as high (from one SNP every 130 bp to one SNP every 20bp). Finally, unlike Stacks, PyRAD allows for indels within loci. The percentage of loci containing indels increases with less stringent sets of parameters (Figure 1l). Depending on the pair of samples considered, this measure varies from a few percent to almost 40 %. For PyRAD, the number of catalogued loci decreased rapidly with the number of specimens included in the analysis (with significant drops corresponding to the number of individuals in the haplotype clades revealed by the phylogenetic reconstruction, see below) (Figure 2). Most loci bore <3 SNPs even when 10 polymorphisms were allowed on a single RAD locus (Figure 2).

We measured the proportion of loci catalogued by Stacks that was also detected by PyRAD using custom BLASTN database searches. Overall, 0.6 to 42.7% of loci detected by Stacks were present in the PyRAD catalog. This pattern is partly explained by the proportion of PyRAD loci with indels (see above), but might also be

influenced by the differential detection of repeated regions (i.e. deleveraging algorithm in Stacks), or the number of reads per individual (the proportion of loci in common between Stacks and PyRAD was lower for individuals with fewer reads; Table 2).

Phylogenetic reconstruction and species delimitation

The automatic boot-stopping method implemented in RAxML yielded 1 000 bootstrap replicates for the mitochondrial phylogeny (91 taxa x 700 nt), 500 replicates for the Stacks RAD phylogenies (91 taxa x 1 080 352 nt, 11 872 loci for the first dataset, and 1 146 054 nt, 12 594 loci for the second dataset), and 200 replicates for the PyRAD phylogeny (91 taxa x 6 120 523 nt, 69 851 loci). The proportion of gaps and undetermined characters ranged between 83 and 84% for Stacks and was 92% for PyRAD. The three RAD phylogenies were similar but not identical, the second Stacks dataset being better resolved than the first, and the PyRAD dataset being better resolved than the Stacks sets (nodes with bootstrap >70%: 19% for m3M4n4, 29% for m3M10n12, 40% for m6s93; Figure 3). Divergence levels were much higher in the RAD phylogenies compared to the mitochondrial phylogeny. For instance, the groups composed of haplotypes 9 and 10 were separated by a distance of 0.001 substitution/site on the *mtMutS* tree, while these clades were separated by 0.27 and 0.25 substitutions/sites on the m3M4n4 and m3M10n12 RAD phylogenies, respectively (Figure 3).

Out of nine mitochondrial haplotypes represented by more than one individual, six formed well-supported monophyletic groups on the RAD phylogenies, for all datasets. One of these clades (corresponding to haplotype 10) contained specimens from both NC and PNG. The group formed by mitochondrial haplotype 7

was polyphyletic on the RAD phylogenies, with specimens grouping in two well-supported clades on the PyRAD phylogeny: one composed of five closely-related NC specimens and one composed of three more divergent PNG colonies (this clade was split in two on the Stacks phylogenies). Specimens characterized by *mtMutS* haplotype 7 may therefore belong to at least three distinct species. On the other hand, specimens characterized by three distinct mitochondrial haplotypes (2, 8, 13) clustered into a single, well-supported clade (with the exception of one individual, TER13034, haplotype 8, which clusters well outside this clade). These three haplotypes, which form a paraphyletic group on the mitochondrial phylogeny and are one to two mutations different from each other, would therefore be considered as one evolutionary unit based on the RAD phylogenies (and population clustering analyses with DAPC and TESS failed to detect structure within this clade; see below). Finally, out of three singleton haplotypes (J, 13, 14), two (J, 14) sit on long branches and are clearly differentiated from other haplotypes using RAD-tag data.

We ran a DAPC on the three clades that contained the most colonies (clade 1: 18 colonies of haplotype 9; clade 2: 20 colonies of haplotype 4; clade 3: 31 colonies of haplotypes 2, 8, 13). Within these clades, 3 685, 1 470 and 8 201 loci were retained (with 25, 42 and 55% missing data, respectively). In all three cases, DAPC failed to detect intra-clade genetic structure, as the most likely number of group (based on BIC, discounting the scenario in which each sample belongs to its own group), in each case, was one (Figure S1). The spatially-explicit admixture model implemented in TESS also failed to detect genetic structure within clades 1 and 3, but suggested the presence of three clusters in clade 2, these clusters being composed of colonies sampled (1) on the slope of New Caledonia, (2) Munida Seamount (Norfolk Ridge), and (3) Jumeaux Ouest Seamount (Norfolk Ridge; Figure S1). The population genetics of *Chrysogorgia* will be further discussed in a separate study.

Detection of environmental contaminants

As octocoral DNA was extracted from whole polyps rather than dissected, internal tissue, some loci may come from environmental contaminants such as bacteria. To evaluate the prevalence of such loci, we blasted all the loci that were catalogued for the m3M4n4 Stacks dataset from individual JAC1018 (n = 1 202). The BLASTN algorithm (Altschul *et al.*, 1997) was used to match RAD loci to the non-redundant NCBI nucleotide database, using 10^{-3} as a statistical significance threshold (e-value). Most sequences (92.6%) could not be assigned to a match in the nucleotide database and 4.5% of loci were similar to bacterial sequences (78-100% similarity between match and query). A single locus matched human mitochondrial DNA (84% similarity); other matches (n = 34) included other invertebrates and plant sequences. Given (1) the small prevalence of potential contaminants, (2) our inability to determine whether these loci really belong to contaminant DNA or correspond to coral sequences which closest matches are non-cnidarian taxa, and (3) the large number of Stacks analyses performed (>400), we decided to run our analyses without trying to filter loci from exogenous DNA sources.

Discussion

A critical decision in RAD analyses is the way the sequencing data are filtered to get to the final SNP dataset. This process goes through several steps to ensure that the final loci will correspond to homologous sequences. The main filters involve several quality filters (sequencing quality, sequencing depth) as well as several similarity thresholds

aimed at identifying the different allelic states of homologous loci. Finally, for each sample, an algorithm is used to tell apart sequencing errors from real mutations in order to conduct the final SNP calling. Even though the overall process is quite similar for Stacks and PyRAD analyses pipelines, a strict comparison of their results is not straightforward since they use sets of parameters that differ to some extent. A main difference between these two pipelines is in the assessment of similarity of loci: Stacks uses a strict similarity criterion (maximum number of mutations) in order to cluster reads into loci, whereas PyRAD uses an overall similarity criterion, after an alignment step, allowing for the presence of indels within clusters. This should be a critical difference when comparing genetically more-distant samples as indels are more likely to occur, and would thus result in sequences being assigned to different loci using Stacks (which will then be excluded from the final catalog since not present in both individuals) while PyRAD would theoretically allow these reads to be considered as homologous loci.

Our results show that more loci are recovered using the PyRAD pipeline. Despite these differences, general trends are similar using both pipelines. First, fewer loci and SNPs are recovered when comparing more genetically distant samples. This result is expected and has been anticipated through simulation (Cariou *et al*. 2013) and observed empirically (Cruaud *et al*. 2014). Our data show an exponential decay of the number of loci recovered as a function of divergence time of samples. Second, the stringency of the filtering process has a significant effect on the number of loci and SNPs identified. Indeed, higher minimum depth of sequencing thresholds and higher similarity threshold lead to fewer loci being identified. This trend is observed regardless of the level of genetic divergence between samples, but it seems to be accentuated when samples are more closely related.

Despite the similarities in general trends, quantitative and qualitative differences are observed in the outputs of each pipeline. Indeed, whatever the set of parameters used, almost twice as many loci are identified using PyRAD compared to Stacks. This difference cannot be solely attributed to the management of indels since our results show that the percentage of loci containing indels is usually around 5-20% and never reaches 40% whatever the genetic distance between samples and the parameters set. Another interesting result is that PyRAD is not simply adding extra loci to the total loci identified by Stacks: only half of the loci identified using Stacks are also present in the PyRAD loci catalogs. It is thus necessary to invoke other filtering processes and differences in algorithm to explain these differences in output. More thorough analyses would be needed in order to identify precisely what are the main sources of divergence in the processing of raw data, in addition to the treatment of indels.

One major result is the remarkable loss of homologous loci with increasing divergence among specimens with different mitochondrial haplotypes. For instance, compared to specimens sharing the same haplotype, specimens two mutations apart at *mtMutS* (estimated divergence of 1-2 My) had on average 70% fewer homologous loci (Stacks analysis at m3M7n8). Within the genus, specimens from mitochondrial clades 16 mutations apart (i.e. the highest divergence level included in our study, estimated between 9 and 16 My) share 97% fewer loci. This rate of loss of homologous RAD-tags is far greater than what has been observed in cetaceans (Viricel *et al.,* 2014), for which 66% of homologous loci were retained at the inter-familial level (short-beaked common dolphins, *Delphinus delphis*, vs. harbour porpoise, *Phocoena phocoena*; estimated divergence of 14-19 My) compared to the intra-specific

480 level (within *Delphinus delphis*). Comparisons within cetaceans were performed using
481 the same custom pipeline as used in the present study, using Stacks parameters
482 m3M3n3 (the results for corals were similar when comparing m3m3n3 to m3M7n8).
483
484 The differences observed between our study and that of Viricel *et al.* (2014)
485 may be explained by various factors. For example, the choice of restriction enzyme
486 was different (*Sbf1* here, *Not1* for Viricel *et al.*), and differences in genome
487 composition (most importantly GC content and size) are unknown. While both studies
488 were conducted with two lanes of Illumina HiSeq2000 sequencing (conducted by
489 Eurofins Genomics in both cases), throughput may have been influenced by the quality
490 of genomic DNA (trawled deep-sea samples here, stranded animals for Viricel *et al.*).
491 These various factors may have significantly influenced the number of cut sites. Our
492 comparisons might also be significantly affected by the precision of the molecular
493 clocks available. Divergence times between cetacean families were inferred based on
494 fossil evidence (see references in Viricel *et al.,* 2014), while no such fossil-calibrated
495 molecular clock exists, to the best of our knowledge, for octocorals. The *mtMutS*
496 divergence rates estimated by Lepard (2003) are based on a group of shallow-water
497 octocorals that may evolve faster than the deep-sea *Chrysogorgia* (a long standing
498 question in deep-sea biology is whether evolutionary process take longer in deeper
499 water, compared to shallower waters; e.g. Wilson and Hessler 1987), and rely on a
500 geological event (rising of the Isthmus of Panama), which can introduce further bias.
501
502 The exploration of divergence parameter space, as outlined above, was made
503 using pairs of specimens, and not allowing any missing data. Stacks and PyRAD can
504 build catalogs with loci shared by a set proportion of individuals within pre-defined
505 groups. Hence, our phylogenetic matrix based on over 12K loci (Stacks parameters

506 m3M10n12) resolved most deeper nodes of the tree despite 83 to 84% of missing
507 data. Similarly, Cruaud *et al.* (2014) constructed a phylogeny of 18 species of the
508 beetle genus *Carabus*, and found that the deepest node of the tree (17 My divergence
509 between species) was characterized by 67% of missing data but strong statistical
510 support. Jones *et al.* (2013) reconstructed phylogenetic relationships among
511 congeneric species of swordtail and platyfish (*Xiphophorus* sp.) that diverged <3 My,
512 and estimated up to 70% missing data (ingroup data; their Table S2). They noted,
513 however, that missing data had little effect on tree topology and branch support. The
514 rate of loss of homologous loci observed in swordtail and platyfish is more on par with
515 what we observed for *Chrysogorgia* than what was reported for cetaceans and *Carabus*
516 beetles, and further emphasizes that (1) the utility of RAD sequencing for phylogenetic
517 reconstruction may be taxon-dependent, and (2) molecular clocks must be critically
518 interpreted. It must be underlined, however, that notable differences in tree
519 topologies were observed between the three inferred RAD phylogenies, such as deep
520 but well-supported nodes (e.g. relative positions of clade 3 and haplotypes 6, 7 and 8).
521
522 RAD-tag sequencing has also proven very useful in testing the criterion used
523 for our primary species delimitation hypotheses, namely that single mitochondrial
524 *mtMutS* haplotypes discriminate species that fit within the General Lineage Concept of
525 species as defined by de Queiroz (1998). Indeed, a large numbers of variable loci could
526 be catalogued within and among closely-related colonies (sharing the same *mtMutS*
527 haplotype, and therefore putatively belonging to the same species) and more
528 distantly-related colonies (separated by 1-16 mutations at *mtMutS*, putatively
529 belonging to different species), allowing us (1) to plot our primary delimitation
530 hypotheses onto well-supported phylogenies, and (2) to explore the spatial structure
531 of populations. Three patterns were evidenced from the data: (1) in the majority of

cases we noted a complete congruence between *mtMutS* haplotypes and RAD clades (6/9 non-singleton haplotypes and 2/3 singleton haplotypes); (2) in one case incomplete congruence was noted (with PyRAD, haplotype 7 corresponding to two RAD clades (one NC, one PNG) that did not form a monophyletic group; (3) in one case a single RAD clade included specimens with different (but closely-related) haplotypes. This result is significant for octocoral taxonomy and systematics, as *mtMutS* has been widely used to assist species delimitation across a large number of families (e.g. review of McFadden *et al.,* 2010). While morphological, mitochondrial (Pante and Watling, 2012) and genomic data (this study) all point to the utility of *mtMutS* for delimiting *Chrysogorgia* species, its resolution should be interpreted in two ways. First, as we did not find 100% congruence between RAD clades and *mtMutS* haplotypes, and tested only a restricted set of putative species, *mtMutS* should still be considered as one of the first steps in an integrative taxonomic loop incorporating more variable markers (e.g. Schlick-Steiner *et al.,* 2010; Kekkonen and Hebert 2014). Second, the evolutionary speed of *mtMutS* may well vary among octocorals, and its resolving power may therefore vary from one group to another (e.g. Baco and Cairns, 2012). Nevertheless, combining mitochondrial markers such as *mtMutS* and RAD-tag data will without doubt be of tremendous value for testing the large number of outdated species hypotheses within the Octocorallia.

Acknowledgments

The authors thank the participants of the national research group "Génomique Environnementale" for stimulating discussions on the use of RAD-tags for inferring phylogenies, in particular R. Debruyne and A. Cruaud. Samples used in this study were

558 collected during the *Terrasses* and *BioPapua* cruises (PIs S. Samadi and L. Corbari) as
559 part of the MNHN/IRD Tropical Deep-Sea Benthos programme (Bouchet *et al.,* 2008),
560 and during the *Extreme Corals 2010* cruise in the northwestern Atlantic (PIs SW Ross
561 and SD Brooke; funding from NOAA's Deep Sea Coral Research and Technology
562 Program). We warmly thank the participants and crew members on these cruises for
563 they indispensable help at sea. This study was funded by the "Institut Écologie et
564 Environnement" of the CNRS ("Appel à Projets en Génomique Environnementale,"
565 organizers Dominique Joly and Denis Faure), the French Muséum national d'Histoire
566 naturelle (Action Thématique du Muséum "Taxonomie moléculaire: DNA Barcode et
567 gestion durable des collections") and by the Agence National de la Recherche (ANR
568 12-ISV7-0005-01 French-Taiwanese project TF-DeepEvo). Parts of the analysis were
569 run on the YMIR super-computer (partly funded by the European Union (contract
570 31031-2008, European Regional Development Fund) of the University of La Rochelle
571 (many thanks to Mikael Guichard, Marc-Henri Boisis-Delavaud and Frédéric Bret). We
572 also thank Julio Pedraza (UMS 2700, MNHN) for his help with bioinformatics. Salary
573 for EP was covered by a grant to the Poitou-Charentes region (Contrat de Projet État-
574 Région 2007- 2013). Finally, the authors thank the editor and two anonymous
575 reviewers for their constructive comments.
576
577 **Conflict of Interest:** The authors declare no conflict of interest.
578
579 **Data Archiving:** Mitochondrial haplotypes were deposited on GenBank (Table S1).
580 Phylogenetic data were deposited on Dryad: doi:xxxxx.
581

582 **References**

583

584 Altschul SF, Madden TL, Schäffer AA, Zhang J, Zhang Z, Miller W, Lipman DJ (1997).
585 Gapped BLAST and PSI-BLAST: a new generation of protein database search.
586 *Nucleic Acids Res* **25**:3389-3402.
587 Baco AR, Cairns SD (2012). Comparing molecular variation to morphological species
588 designations in the deep-sea coral *Narella* reveals new insights into seamount
589 coral ranges. *PLoS ONE* **7**: e45555.
590 Baird NA, Etter PD, Atwood TS, Currey MC, Shiver AL, Lewis ZA, *et al.* (2008). Rapid
591 SNP discovery and genetic mapping using sequenced RAD markers. *PLoS ONE* **3**:
592 e3376.
593 Bouchet P, Héros V, Lozouet P, Maestrati P (2008). A quarter-century of deep-sea
594 malacological exploration in the South and West Pacific: Where do we stand? How
595 far to go? In: Héros V, Cowie RH, Bouchet P (eds), *Tropical Deep-Sea Benthos* 25.
596 vol. **196**, pp. 9–40.
597 Calderón I, Garrabou J, Aurelle D (2006). Evaluation of the utility of COI and ITS
598 markers as tools for population genetic studies of temperate gorgonians. *J Exp*
599 *Mar Biol Ecol* **336**: 184–197.
600 Cariou M, Duret L, Charlat S (2013). Is RAD-Seq suitable for phylogenetic inference? an
601 *in silico* assessment and optimization. *Ecol Evol* **3**: 846–852.
602 Catchen J, Hohenlohe PA, Bassham S, Amores A, Cresko WA (2013). Stacks: an analysis
603 tool set for population genomics. *Mol Ecol* **22**: 3124–3140.
604 Concepcion GT, Crepeau M, Toonen RJ (2008). An alternative to ITS, a hypervariable,
605 single-copy nuclear intron in corals, and its use in detecting cryptic species within
606 the octocoral genus *Carijoa*. *Coral Reefs* **27**: 323–336.

607 Cruaud A, Gautier M, Galan J M Foucaud, Sauné L, Genson G, Dubois E, *et al.* (2014).
608 Empirical Assessment of RAD sequencing for interspecific phylogeny. *Mol Biol*
609 *Evol* **31**: 1272–1274.
610 Davey JW, Hohenlohe PA, Etter PD, Boone JQ, Catchen JM, Blaxter ML (2011). Genome-
611 wide genetic marker discovery and genotyping using next-generation sequencing.
612 *Nat Rev Genet* **12**: 499–510.
613 de Queiroz K (1998). The General Lineage Concept of Species, Species Criteria, and the
614 Process of Speciation. In: Howard DJ, Berlocher SH (eds) *Endless Forms: Species*
615 *and Speciation*. Oxford University Press, pp 57-75.
616 Dueñas L, Sánchez J (2009). Character lability in deep-sea bamboo corals
617 (Octocorallia, Isididae, Keratoisidinae). *Mar Ecol Prog Ser* **397**: 11–23.
618 Durand E, Jay F, Gaggiotti OE, François O (2009). Spatial inference of admixture
619 proportions and secondary contact zones. *Mol Biol Evol* **26**: 1963–1973.
620 Eaton D (2014). PyRAD: assembly of *de novo* RADseq loci for phylogenetic analyses.
621 *Bioinformatics* **30**:1844-1849.
622 Eaton DAR, Ree RH (2013). Inferring phylogeny and introgression using RADseq data:
623 an example from flowering plants (Pedicularis: Orobanchaceae). *Syst Biol* **62**:
624 689–706.
625 Ekblom R, Galindo J (2011). Applications of next generation sequencing in molecular
626 ecology of non-model organisms. *Heredity* **107**: 1–15.
627 France SC (2007). Genetic analysis of bamboo corals (Cnidaria: Octocorallia: Isididae):
628 does lack of colony branching distinguish *Lepidisis* from *Keratoisis*? *Bull Mar Sci*
629 **81**: 323–333.
630 France SC, Rosel PE, Agenbroad JE, Mullineaux LS, Kocher TD (1996). DNA sequence
631 variation of mitochondrial large-subunit rRNA provides support for a two-

632 subclass organization of the Anthozoa (Cnidaria). *Mol Mar Biol Biotechnol* **5**: 15–
633 28.
634 Gregory TR (2014). *Animal genome size database*. URL: http://www.genomesize.com
635 Gruenthal KM, Witting DA, Ford T, Neuman MJ, Williams JP, Pondella DJ, Bird A,
636 Caruso N, Hyde JR, Seeb LW, Larson WA (2014). Development and application of
637 genomic tools to the restoration of green abalone in southern California. *Conserv*
638 *Genet* **15**:109–121.
639 Herrera S, Baco A, Sánchez JA (2010). Molecular systematics of the bubblegum coral
640 genera (Paragorgiidae, Octocorallia) and description of a new deep-sea species.
641 *Mol Phylogenet Evol* **55**: 123–135.
642 Jombart T (2008). adegenet: a R package for the multivariate analysis of genetic
643 markers. *Bioinformatics* **24**: 1403–5.
644 Jombart T, Devillard S, Balloux F (2010). Discriminant analysis of principal
645 components: a new method for the analysis of genetically structured populations.
646 *BMC Genetics* **11**.
647 Jones JC, Fan S, Franchini P, Schartl M, Meyer A (2013). The evolutionary history of
648 *Xiphophorus* fish and their sexually selected sword: a genome-wide approach
649 using restriction site-associated DNA sequencing. *Mol Ecol* **22**: 2986-3001.
650 Kekkonen M, Hebert PD (2014). DNA barcode-based delineation of putative species:
651 efficient start for taxonomic workflows. *Mol Ecol Res* **14**:706-15.
652 Leaché AD, Fujita MK, Minin VN, Bouckaert RR (2014). Species delimitation using
653 genome-wide SNP data. Syst Biol 63:534-542.
654 Lepard A (2003). *Analysis of variation in the mitochondrial encoded msh1 in the genus*
655 Lepidogorgia *(Cnidaria: Octocorallia) and implications for population and*
656 *systematics studies*. Master's thesis, College of Charleston, Charleston, SC.

Lexer C, Mangili S, Bossolini E, Forest F, Stölting KN, Pearman PB, *et al.* (2013). 'Next generation' biogeography: towards understanding the drivers of species diversification and persistence. *J Biogeogr* **40**: 1013–1022.

McFadden CS, Benayahu Y, Pante E, Thoma JN, Nevarez PA, France SC (2011). Limitations of mitochondrial gene barcoding in Octocorallia. *Mol Ecol Res* **11**: 19–31.

McFadden CS, Sánchez JA, France SC (2010). Molecular phylogenetic insights into the evolution of Octocorallia: A review. *Integr Comp Biol* **50**: 389–410.

Miller M, Pfeiffer W, Schwartz T (2010). Creating the CIPRES Science Gateway for inference of large phylogenetic trees. In: *Proceedings of the Gateway Computing Environments Workshop (GCE)*. New Orleans, LA, United States, pp. 1–8.

Mokhtar-Jamaï K, Pascual M, Ledoux JB, Coma R, Féral JP, Garrabou J, *et al.* (2011). From global to local genetic structuring in the red gorgonian *Paramuricea clavata*: the interplay between oceanographic conditions and limited larval dispersal. *Mol Ecol* **20**: 3291–3305.

Nadeau NJ, Martin SH, Kozak KM, Salazar C, Dasmahapatra K, Davey JW, *et al.* (2013). Genome-wide patterns of divergence and gene flow across a butterfly radiation. *Mol Ecol* **22**: 814–826.

Pante E, Corbari L, Thubaut J, Chan TY, Mana R, Boisselier MC, *et al.* (2012a). Exploration of the deep-sea fauna of Papua New Guinea. *Oceanography* **25**: 214–225.

Pante E, France S, Couloux A, Cruaud C C McFadden, Samadi S, Watling L (2012b). Deep-sea origin and in-situ diversification of chrysogorgiid octocorals. *PLoS ONE* **7**: e38357.

Pante E, France SC (2010). *Pseudochrysogorgia bellona* n. gen. n. sp.: a new genus and species of chrysogorgiid octocoral (Coelenterata: Anthozoa) from the Coral Sea. *Zoosystema* **32**: 595–612.

Pante E, Watling L (2012). *Chrysogorgia* from the New England and Corner Seamounts: Atlantic – Pacific connections. *J Mar Biol Assoc U.K.* **92**: 911–927.

Puillandre N, Modica MV, Zhang Y, Sirovich L, Boisselier MC, Cruaud C, Holford M, Samadi S (2012). Large-scale species delimitation method for hyperdiverse groups. *Mol Ecol* **21**:2671-2691.

R Development Core Team (2014). *R: A Language and Environment for Statistical Computing*. R Foundation for Statistical Computing, Vienna, Austria. ISBN 3-900051-07-0. URL: http://www.R-project.org

Reitzel AM, Herrera S, Layden MJ, Martindale MQ, Shank TM (2013). Going where traditional markers have not gone before: Utility of and promise for RAD sequencing in marine invertebrate phylogeography and population genomics. *Mol Ecol* **22**:2953-2970.

Rubin BER, Ree RH, Moreau CS (2012). Inferring phylogenies from RAD sequence data. *PLoS ONE* **7**: e33394.

Schlick-Steiner BC, Steiner FM, Seifert B, Stauffer C, Christian E, Crozier RH (2010). Integrative taxonomy: a multisource approach to exploring biodiversity. *Annu Rev Entomol* **55:**421-438.

Soza-Ried J, Hotz-Wagenblatt A, Glatting K-H, del Val C, Fellenberg K, Bode HR, Frank U, Hoheisel JD, Frohme M (2010). The transcriptome of the colonial marine hydroid *Hydractinia echinata*. *FEBS Journal* **277**:197–209.

Stamatakis A (2006). RAxML-VI-HPC: Maximum likelihood-based phylogenetic analyses with thousands of taxa and mixed models. *Bioinformatics* 22: 2688–2690.

706 Stamatakis A, Hoover P, Rougemont J (2008). A rapid bootstrap algorithm for the
707 RAxML web servers. *Syst Biol* **57**: 758–771.
708 Taylor JW, Jacobson DJ, Kroken S, Kasuga T, Geiser DM, Hibbett DS, Fisher MC (2000).
709 Phylogenetic species recognition and species concepts in fungi. *Fungal Genet Biol*
710 **31**:21-32.
711 Viricel A, Pante E, Dabin W, Simon-Bouhet B (2014). Applicability of RAD-tag
712 genotyping for interfamilial comparisons: empirical data from two cetaceans. *Mol*
713 *Ecol Res* **14**: 597–605.
714 Vollmer S, Palumbi S (2004). Testing the utility of internally transcribed spacer
715 sequences in coral phylogenetics. *Mol Ecol* **13**: 2763–2772.
716 Wagner CE, Keller I, Wittwer S, Selz OM, Mwaiko S, Greuter L, *et al.* (2013). Genome-
717 wide RAD sequence data provide unprecedented resolution of species boundaries
718 and relationships in the Lake Victoria cichlid adaptive radiation. *Mol Ecol* **22**:
719 787–798.
720 Watling L, France SC, Pante E, Simpson A (2011). Biology of deep-water octocorals.
721 *Adv Mar Biol* **60**: 41–123.
722 Wilson GDF, Hessler R (1987). Speciation in the Deep Sea. *Annu Rev Ecol Evol Syst*
723 **18**:185-207.
724 Zhang Z, Schwartz S, Wagner L, Miller W (2000). A greedy algorithm for aligning DNA
725 sequences. *J Comput Biol* **7**: 203–214.
726

Titles and Legends to Figures

Figure 1. Comparison of locus detection for Stacks (a-f) and PyRAD (g-l). The number of loci, SNPs and indels detected for specimens separated by 0-16 mutations at the mitochondrial *mtMutS* gene are shown for the different read coverage (m parameter) and divergence levels (M and n parameters, see text). In PyRAD analyses, "s" corresponds to the "Wclust" parameter.

Figure 2. Information content of the locus catalog built by PyRAD for all 91 *Chrysogorgia* specimens. Wclust: percent divergence permitted between loci within and across specimens; in addition to the 93% Wclust level used to infer the *Chrysogorgia* phylogeny, the 89% Wclust level was tested here.

Figure 3. Maximum likelihood phylogenetic trees inferred using RAxML for the mitochondrial *mtMutS* data (a), and RAD loci (b-d). Bootstrap node support (1000 replicates for a, 500 replicates for b-c, 200 for d) is presented only for nodes with ≥ 70% support. At the tips, colored dots, which represent *mtMutS* haplotype membership (each color represents a unique haplotype), are followed by specimen identifiers and haplotype numbers. Each tree was rooted to the Atlantic specimen (JAC1018, haplotype J). Genetic structure within clades 1, 2 and 3 were further investigated using a DAPC and TESS (see text and Figure S1). Scale bars: substitution / site.

Figure S1. Population genetic structure within three clades of the phylogenetic analysis. a-c: Bayesian Information Criterium (BIC) values for each tested number of DAPC cluster. For each clade, the maximum number of clusters was set as the

753 number of individuals minus one (a: clade 1, b: clade 2,c: clade 3). d-e: Boxplots of
754 Deviance Information Criterion (DIC) values for each value of K. g: Longer TESS
755 analysis (12 000 MCMC steps) performed on clade 2 colonies, for K=3. g: On the
756 left, the phylogenetic relationships between colonies within clade 2 are
757 represented based on the PyRAD dataset, and colored squared at the tips
758 represent geography (orange: Jumeau Ouest Seamount, green: Munida Seamount,
759 blue: New Caledonia slope). On the right, q values (ancestry proportions inferred
760 from the CAR admixture model) are given for each individual from clade 2.
761
762 **Table 1.** Summary table of haplotype information (sample size, geographical spread,
763 depth range, habitat (seamounts vs. slopes) and *mtMutS* vs. RAD delimitation. NC:
764 New Caledonia, PNG: Papua New Guinea
765
766 **Table 2.** Results of the BLASTN alignments performed between Stacks and PyRAD
767 sequences. The number of loci detected within nine individuals (with high,
768 medium and low read numbers) is presented for the two analyses performed on
769 the entire set of 91 specimens. The number of quality-filtered reads is given in
770 million.
771
772 **Table S1.** Excel table with information on collection (location, date, coordinates,
773 depth), mitochondrial haplotypes (haplotype number and GenBank accession
774 number), and number of quality-filtered reads for the 91 *Chrysogorgia* specimens
775 used in this study. The 6-9 nucleotide barcodes used to distinguish specimens
776 after Illumina sequencing are also included.

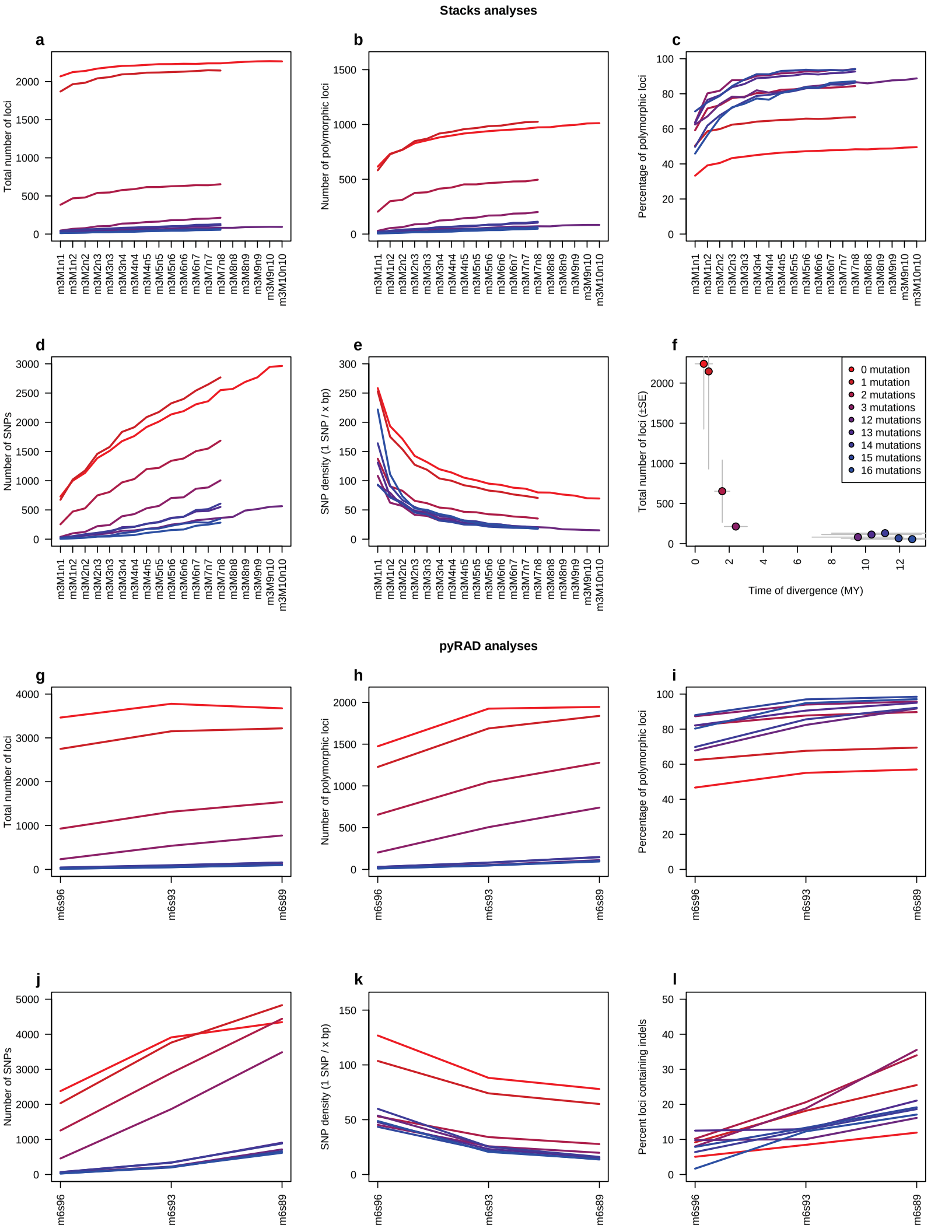
Stacks analyses
a
Total number of loci
b
Number of polymorphic loci
c
Percentage of polymorphic loci
d
Number of SNPs
e
SNP density (1 SNP / x bp)
f
Total number of loci (±SE)
0 mutation
1 mutation
2 mutations
3 mutations
12 mutations
13 mutations
14 mutations
15 mutations
16 mutations
Time of divergence (MY)
m3M1n1
m3M1n2
m3M2n2
m3M2n3
m3M3n3
m3M3n4
m3M4n4
m3M4n5
m3M5n5
m3M5n6
m3M6n6
m3M6n7
m3M7n7
m3M7n8
m3M8n8
m3M8n9
m3M9n9
m3M9n10
m3M10n10
pyRAD analyses
g
Total number of loci
h
Number of polymorphic loci
i
Percentage of polymorphic loci
j
Number of SNPs
k
SNP density (1 SNP / x bp)
l
Percent loci containing indels
m6s96
m6s93
m6s89

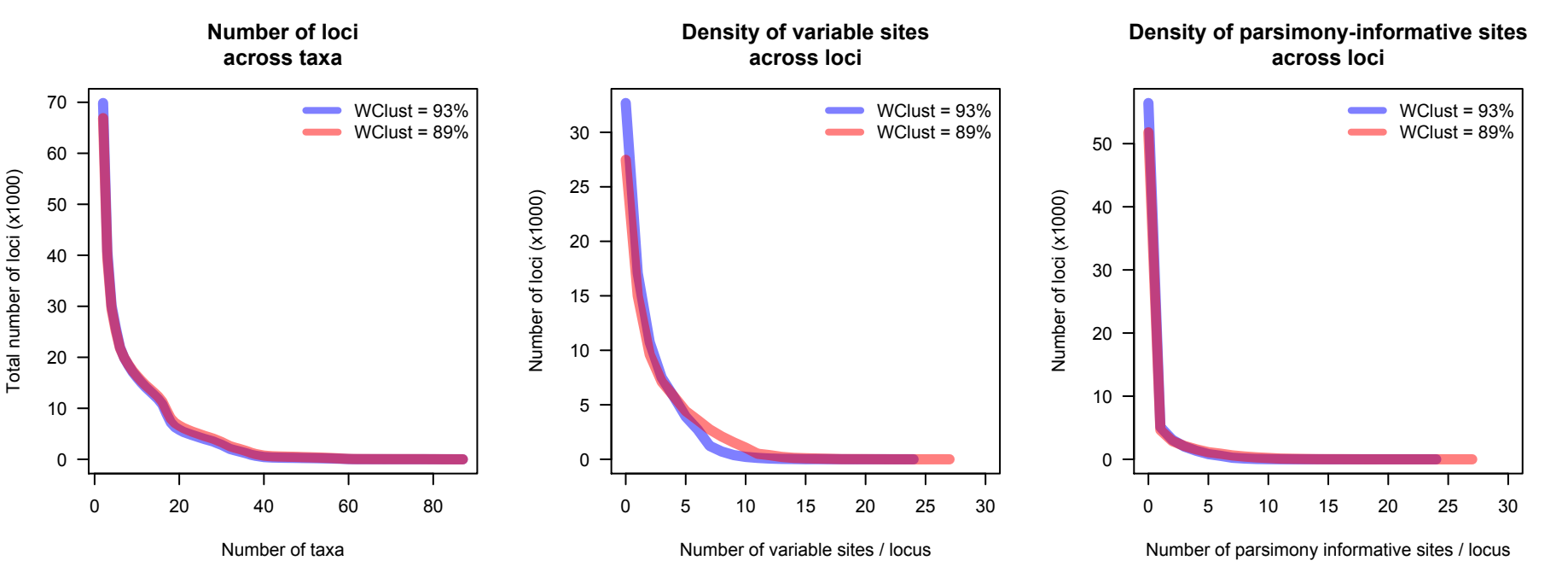
Number of loci
across taxa
Total number of loci (x1000)
Number of taxa
WClust = 93%
WClust = 89%
0
10
20
30
40
50
60
70
0
20
40
60
80
Density of variable sites
across loci
Number of loci (x1000)
Number of variable sites / locus
WClust = 93%
WClust = 89%
0
5
10
15
20
25
30
0
5
10
15
20
25
30
Density of parsimony-informative sites
across loci
Number of loci (x1000)
Number of parsimony informative sites / locus
WClust = 93%
WClust = 89%
0
10
20
30
40
50
0
5
10
15
20
25
30

a. Mitochondrial, *mtMutS*

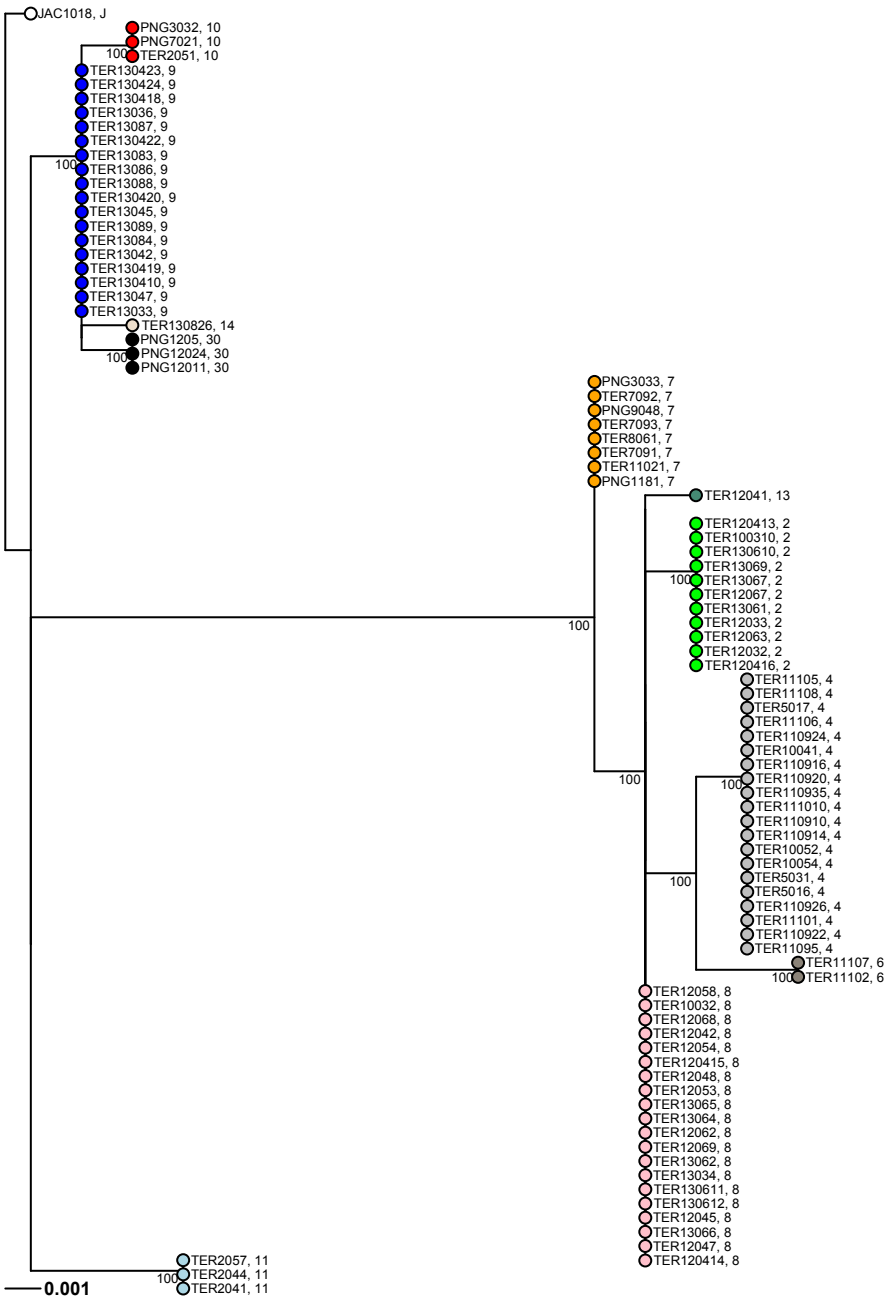

b. RAD-tags, Stacks m3M4n4 dataset

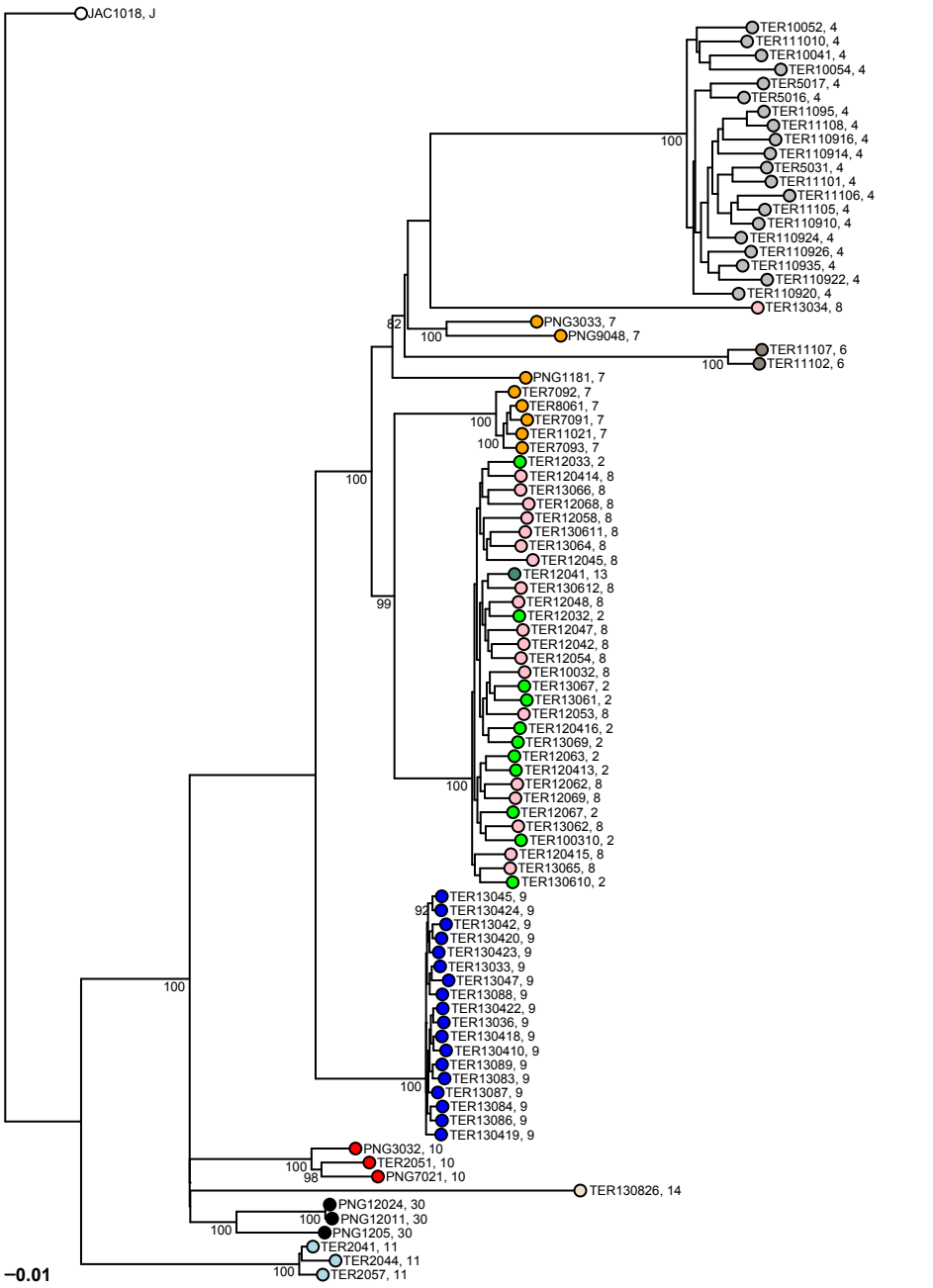

c. RAD-tags, Stacks m3M10n12 dataset

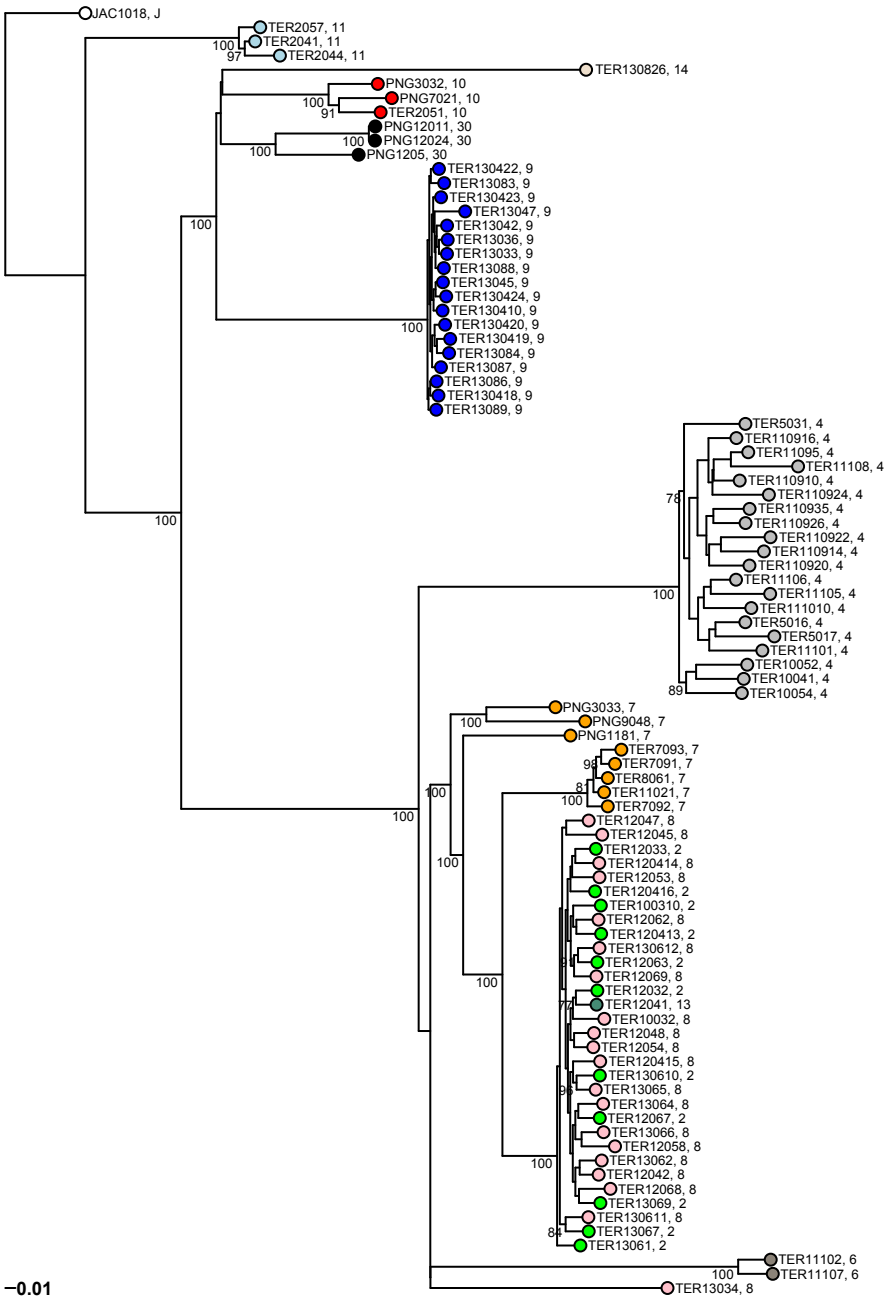

d. RAD-tags, PyRAD m6s93 dataset

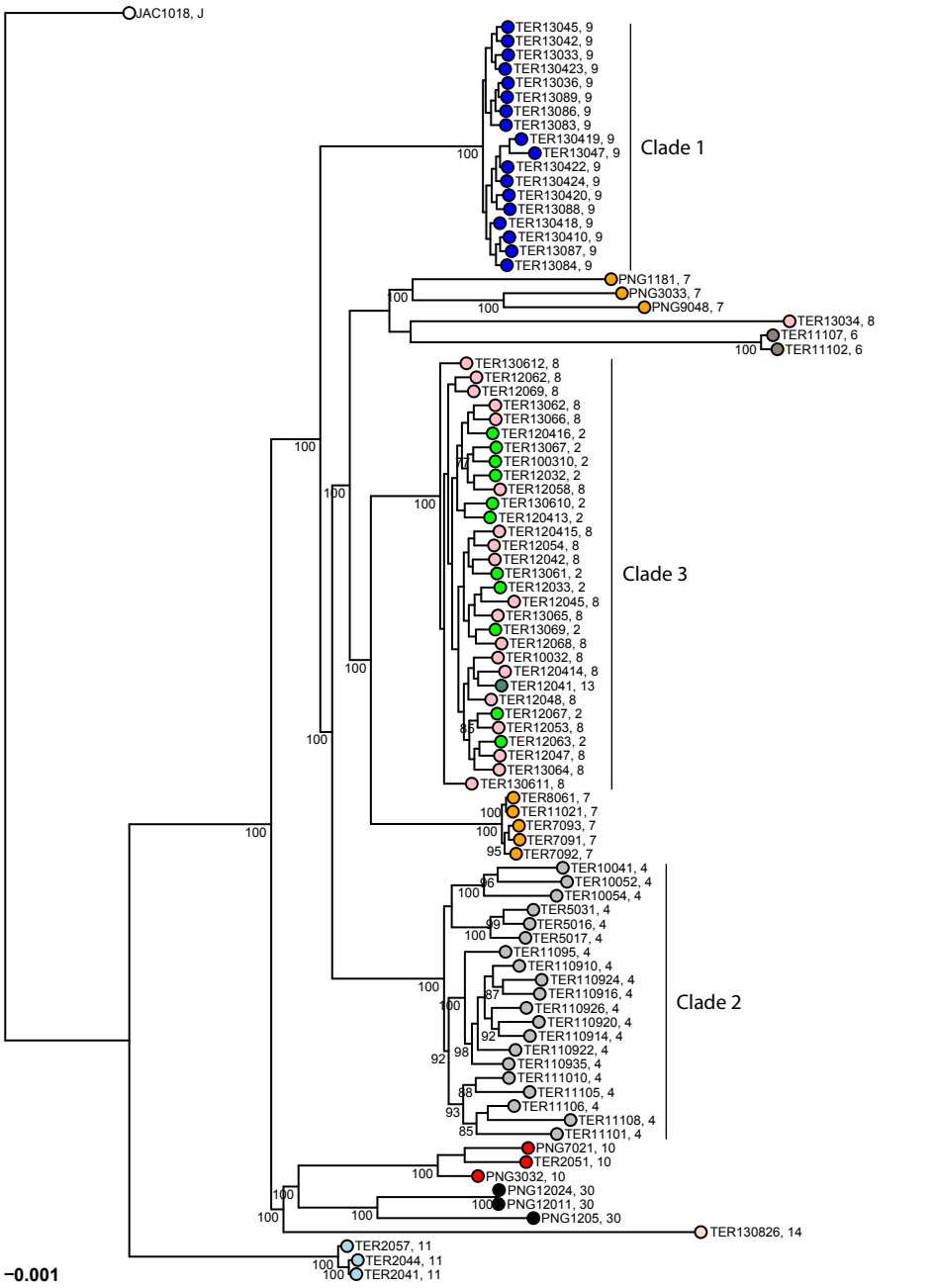

Haplotype	N. colonies	Geography	Habitat	Depth range (m)
J	1	Atlantic	slope	627 - 627
2	11	NC	slope	390 - 500
4	20	NC	slope & seamoun	150 - 330
6	2	NC	seamount	270 - 310
7	8	NC-PNG	slope & seamoun	300 - 880
8	20	NC	slope	390 - 500
9	18	NC	slope	390 - 450
10	3	NC	slope & seamoun	458 - 880
11	3	NC	seamount	750 - 840
13	1	NC	slope	460 - 490
14	1	NC	slope	400 - 420
30	3	PNG	slope	220 - 1020

Delimitation
mtMutS / RAD congruence
mtMutS / RAD incongruence
mtMutS / RAD congruence
mtMutS / RAD congruence
mtMutS / RAD incongruence
mtMutS / RAD incongruence
mtMutS / RAD congruence
mtMutS / RAD congruence
mtMutS / RAD congruence
mtMutS / RAD incongruence
mtMutS / RAD congruence
mtMutS / RAD congruence

				89% divergence	
Specimen	**Haplotype**	**read.category**	**N. reads (M)**	**N. loci (pyRAD)**	**N. loci (Stacks)**
TER2044	11	high	5.82	6580	866
JAC1018	J	high	5.49	3305	1851
TER7092	7	high	4.04	6867	1363
TER130424	9	median	1.61	6151	1198
TER13064	8	median	1.61	6876	4183
TER13087	9	median	1.60	5959	1131
TER11101	4	low	0.09	1046	228
TER13047	9	low	0.08	1145	396
TER11108	4	low	0.04	441	50

	93% divergence		
Intersect (%)	**N. loci (pyRAD)**	**N. loci (Stacks)**	**Intersect (%)**
7.84	6720	607	5.54
24.57	2717	1202	21.46
13.03	6862	1246	11.40
12.73	6323	850	8.86
39.89	6584	4607	42.72
13.81	6189	821	9.26
1.15	944	138	0.64
9.96	1107	297	8.67
2.49	384	32	1.04